



ELSEVIER

Physica C 252 (1995) 13–21

PHYSICA C

Single-crystal growth and characterization of $\text{REBa}_2\text{Cu}_4\text{O}_8$ and $\text{Y}_{1-x}\text{Ca}_x\text{Ba}_2\text{Cu}_4\text{O}_8$

C.A. Hajar^{a,b}, C.L. Stern^a, K.R. Poeppelmeier^{a,b,*}, K. Rogacki^{c,1}, Z. Chen^c,
B. Dabrowski^c

^a Department of Chemistry, Northwestern University, Evanston, IL 60208, USA

^b The Science and Technology Center for Superconductivity, Northwestern University, Evanston, IL 60208, USA

^c Department of Physics and The Science and Technology Center for Superconductivity, Northern Illinois University,
DeKalb, IL 60115, USA

Received 22 May 1995; revised manuscript received 27 July 1995

Abstract

Crystals of $\text{REBa}_2\text{Cu}_4\text{O}_8$ (RE = Yb, Tm, Er, Ho, Dy, and $\text{Y}_{1-x}\text{Ca}_x$) were grown at 1100°C and 600 bar of O_2 pressure in a hot isostatic press furnace. Single crystal X-ray diffraction data show that all compounds crystallized in space group Ammm (#65) with the approximate lattice parameters $a \approx 3.82$ Å, $b \approx 3.86$ Å, $c \approx 27.1$ Å, and $Z = 2$. As the ionic radius of the lanthanide decreased, the lattice parameters decreased. Substitution of calcium in $\text{Y}_{1-x}\text{Ca}_x\text{Ba}_2\text{Cu}_4\text{O}_8$ crystals ($x \sim 0.02$) increased T_c to 87 K.

1. Introduction

The structure and properties of $\text{YBa}_2\text{Cu}_3\text{O}_{7-\delta}$ (Y123) has been extensively studied in order to understand the mechanism of high-temperature superconductivity [1–3]. One drawback of Y123 is its instability as the temperature is increased [4]; that is Y123 loses oxygen and transforms from an orthorhombic to a tetragonal structure. This transformation makes untwinned single crystals, necessary for detailed measurement of anisotropic physical properties, difficult to prepare. The related high- T_c superconductor $\text{YBa}_2\text{Cu}_4\text{O}_8$ (Y124, $T_c \sim 80$ K) is,

however, quite stable with respect to its oxygen content and structure [5], which results in reproducible oxygen contents and transition temperatures (T_c) for different samples and eliminates the need for the detwinning procedures.

Studies of Y124 have not been as extensive as those for Y123, owing to its later discovery and the need to prepare it at high oxygen pressures. As in the 123 system, most of the lanthanides can substitute for the yttrium in Y124. Polycrystalline samples of $\text{REBa}_2\text{Cu}_4\text{O}_8$ (RE = Nd, Sm, Eu, Gd, Dy, Y, Ho, Er, and Tm) have been prepared and studied by several groups [6–8]. Each noted the correlation between the atomic radius of the lanthanide and the critical temperature; as the radius increased, the T_c decreased. Unlike Y123, attempts to increase the T_c by doping have been successful. Calcium can be doped onto the yttrium site with a solubility limit

* Corresponding author.

¹ Permanent address: Institute of Low Temperature and Structural Research, Polish Academy of Sciences, 50-950 Wrocław, Poland.

approaching 10% for the polycrystalline material [9]. At this concentration, the T_c increases from 80 K to 90 K. While the structures of the compounds listed above have all been determined via powder X-ray diffraction, only Y124 [10,11], Dy124 [12], and $Y_{1-x}Ca_x$ 124 [13] have been analyzed by single crystal X-ray diffraction.

Owing to the incongruent melting behavior of RE124 compounds, flux techniques are commonly used to grow single crystals [14]. At growth temperatures of about 1100°C, a high oxygen pressure is needed to suppress decomposition to the Y123 phase [15]. Y124 single crystals have been grown in Al_2O_3 [5,11,15] and ZrO_2 [11] crucibles from a self-flux based on the BaO–CuO eutectic and recently Ca doped Y124 crystals were synthesized in Al_2O_3 crucibles [13]. In contrast to pure Y124 crystals, incorporation of aluminum from the crucible resulted in reduced and sample-dependent transition temperatures (T_c). In this paper, we present crystal-structure data for six RE124 crystals (RE = Yb, Tm, Er, Ho, Dy, and $Y_{1-x}Ca_x$) prepared in ZrO_2 crucibles at 1100°C and 600 bar O_2 pressure. No evidence was detected for the incorporation of zirconium from the crucible, therefore crystals with reproducible properties were grown. The T_c versus ionic size of the lanthanide cations was found to be similar to that reported earlier for polycrystalline samples [6–8]. The calcium solubility for Y124 at 1100°C is smaller than that reported for polycrystalline materials. Our refinements indicated that calcium was not located on the Ba site and was therefore in agreement with a recent report by Fischer et al. [16].

2. Experimental

2.1. Crystal growth

The high-pressure growths of RE124 single crystals were performed from flux using mixtures of polycrystalline RE123 (RE = Nd, Sm, Eu, Gd, Dy, Ho, Er, Tm, Yb, and Lu), $BaCuO_2$, and CuO. The calcium-substituted Y124 crystals were grown from a mixture of $Y_{0.8}Ca_{0.2}Ba_2Cu_3O_7$, $BaCuO_2$ and CuO. Polycrystalline starting materials were synthesized from oxides and carbonates (> 99.9% pure) in flowing oxygen at 900°C, followed by slow cooling to

room temperature. RE123, or $Y_{0.8}Ca_{0.2}Ba_2Cu_3O_7$, $BaCuO_2$, and CuO were mixed in appropriate ratios to obtain the starting compositions with a metal ratio of RE : Ba : Cu \sim 1 : 8 : 20 for RE124 and Y : Ca : Ba : Cu \sim 0.8 : 0.2 : 8 : 20 for the calcium-substituted Y124. The Y : Ba : Cu \sim 1 : 8 : 20 composition was previously found to yield the best crystals in the case of Y124 [11]. Additional mixtures with RE : Ba : Cu \sim 1 : 14 : 35 were also made for RE = Nd, Sm, and Dy. The pre-fired master batch of $REBa_8Cu_{20}O_x$ (\sim 100 g) was pressed into pellets and placed into yttrium-stabilized-zirconium-oxide (YSZ) cylindrical crucibles with 20 cm³ capacity. Unpressed powder was used to cover the pellets and to fill any remaining cavities between the solid pieces.

High-pressure crystal growths were completed in a 20% O_2 /Ar atmosphere at a total pressure of 3 kbar (600 bar O_2 pressure) using a hot isostatic press furnace. This large capacity furnace (inside diameter 8 cm and height 16 cm) is very convenient for crystal growths from flux because it can accommodate several large-size samples in one run. Several crucibles were placed side-by-side in the vertical furnace and the system was purged three times with reaction gas to remove nitrogen, carbon dioxide and moisture from the reaction chamber. The system was then pressurized to $P(O_2) \sim$ 200 bar (\sim 1 kbar total pressure) at room temperature. The temperature was raised to 1100°C at 12°C/min, causing the $P(O_2)$ to increase to 600 bar. The temperature was held at 1100°C for 0.5 h, then slowly decreased to 1060°C at 5°C/h, followed by cooling to room temperature at 60°C/h with the oxygen pressure gradually decreasing to 200 bar. The pressure was released at room temperature and the crucibles were removed for examination.

During crystal growth, the starting mixture partially melted. The remaining sintered mass had a smooth surface with a gap near the crucible wall. After breaking the crucibles, cavities were observed in this gap region for RE = Yb, Tm, Er, Ho, Dy, and Gd. Nearly free-standing, millimeter-size crystals with shiny surfaces were located inside the cavities. Crystals were easy to remove using forceps. No crystals were recovered for RE = Lu, Eu, Sm, and Nd. Additional attempts to grow crystals of Nd, Sm, and Eu at 1080°C using the lower melting starting composition 1 : 14 : 35 were unsuccessful.

2.2. Crystal characterization

All crystals showed a plate-like morphology with the longer dimension in the basal plane. In most cases the crystals grew into bar-like shapes. Using polarizing-light microscopy the longer dimension of the bar-like crystals was assigned to the *b*-axis (along the double-chain direction) analogous to Y123 crystals. The surfaces showed only one orthorhombic domain. However, some crystals were observed with twinning along the *c*-axis. These crystals showed several domains with a 90° misorientation of the *a*-axis along the *c*-axis direction. Twin free crystals were chosen for further structural characterization. No untwinned crystals of Gd124 that were suitable for single crystal X-ray diffraction were found. Elemental analysis was performed using a Hitachi Scanning Electron Microscope (SEM) equipped with an Energy Dispersive X-ray Analyzer (EDAX).

2.3. Crystallographic data and structure determination

Crystal data were collected for the six compounds REBa₂Cu₄O₈ (RE = Yb, Tm, Er, Ho, Dy, and Y_{1-x}Ca_x) (see Table 1). All measurements were made on an Enraf-Nonius CAD4 diffractometer with graphite monochromated Mo Kα radiation ($\lambda = 0.71069 \text{ \AA}$) at a temperature of -120°C . The crystals were black rectangular platelets with the faces {100}, {010}, and {001}, and the dimensions listed. The compounds crystallized in the orthorhombic space group Ammm (#65) and gave the approximate lattice parameters $a \approx 3.82 \text{ \AA}$, $b \approx 3.86 \text{ \AA}$, and $c \approx 27.1 \text{ \AA}$. These parameters were obtained from 25 carefully centered reflections in the range $22.4 < 2\theta < 27.5^\circ$. The maximum 2θ value for the data collection was 80° , and the intensities of three standard reflections measured every 90 min remained constant.

Table 1
Crystallographic data for RE124

	Formula					
	YbBa ₂ Cu ₄ O ₈	TmBa ₂ Cu ₄ O ₈	ErBa ₂ Cu ₄ O ₈	HoBa ₂ Cu ₄ O ₈	DyBa ₂ Cu ₄ O ₈	Y _{0.98} Ca _{0.02} Ba ₂ Cu ₄ O ₈
fw (g/mole)	829.88	825.77	824.10	821.77	819.34	740.86
Cryst. system	orthorhombic	orthorhombic	orthorhombic	orthorhombic	orthorhombic	orthorhombic
Space group	Ammm	Ammm	Ammm	Ammm	Ammm	Ammm
Lattice param.						
<i>a</i> (Å)	3.8213 (9)	3.822 (1)	3.8255 (6)	3.832 (1)	3.833 (1)	3.8344 (6)
<i>b</i> (Å)	3.859 (1)	3.856 (2)	3.860 (1)	3.8651 (6)	3.864 (1)	3.8640 (8)
<i>c</i> (Å)	27.109 (6)	27.113 (9)	27.110 (6)	27.128 (7)	27.115 (7)	27.156 (6)
Volume (Å ³)	399.8 (3)	399.6 (4)	400.3 (3)	401.8 (3)	401.6 (4)	402.3 (2)
<i>b/a</i>	1.0099	1.0089	1.0090	1.0086	1.0081	1.0077
<i>z</i>	2	2	2	2	2	2
<i>R</i> ^a	0.049	0.051	0.047	0.048	.026	0.042
<i>R</i> _w ^a	0.065	0.065	0.066	0.070	.033	0.055
μ (Mo Kα) (cm ⁻¹)	317.40	313.04	306.70	299.38	293.72	265.83
Trans. factor	0.03–0.57	0.16–0.73	0.16–0.78	0.01–0.19	0.05–0.63	0.04–0.63
Secondary ext.	0.94881E-05	0.33233E-05	0.10147E-06	0.88755E-04	0.18416E-05	0.59084E-05
# Reflections	1623	1700	1627	3365	1710	2128
Unique $I > 3\sigma$	715	707	707	712	698	839
Calc. ρ (g/cm ³)	6.894	6.863	6.836	6.792	6.775	6.115
Crystal dimen. (mm)	0.350 × 0.160 × 0.013	0.340 × 0.130 × 0.020	0.515 × 0.146 × 0.007	0.500 × 0.460 × 0.080	0.257 × 0.188 × 0.016	0.290 × 0.190 × 0.013

^a $R = \sum \|F_o\| - |F_c| / \sum \|F_o\|$; $R_w = [(\sum_w (|F_o| - |F_c|)^2 / \sum_w F_o^2)]^{1/2}$.

Table 2
Atomic positions for RE124^a

Atom	Site	x	y	z	YbBa ₂ Cu ₄ O ₈		TmBa ₂ Cu ₄ O ₈		ErBa ₂ Cu ₄ O ₈		HoBa ₂ Cu ₄ O ₈		DyBa ₂ Cu ₄ O ₈		Y _{0.98} Ca _{0.02} Ba ₂ Cu ₄ O ₈	
					B _{eq}	z	B _{eq}	z								
Ln	2c	0.5	0.5	0.0	0.21(2)	0.0	0.0	0.16(2)	0.0	0.18(2)	0.0	0.25(2)	0.0	0.23(1)	0.0	0.24(2)
Ba	4j	0.5	0.5	0.13438(2)	0.24(2)	0.13455(2)	0.20(2)	0.13461(2)	0.29(2)	0.13475(2)	0.22(2)	0.13475(2)	0.28(1)	0.13487(1)	0.13468(1)	0.29(1)
Cu1	4i	0.0	0.0	0.21284(5)	0.26(4)	0.21288(5)	0.22(4)	0.21289(5)	0.31(4)	0.21288(4)	0.24(4)	0.21288(4)	0.33(2)	0.21298(3)	0.21289(3)	0.34(2)
Cu2	4i	0.0	0.0	0.06055(5)	0.19(4)	0.06097(6)	0.13(2)	0.06119(6)	0.21(2)	0.06142(5)	0.15(4)	0.06142(5)	0.19(2)	0.06173(3)	0.06150(3)	0.26(2)
O1	4i	0.0	0.0	0.1450(3)	0.4(2)	0.1449(3)	0.3(2)	0.1445(4)	0.6(1)	0.1459(3)	0.5(1)	0.1459(3)	0.6(1)	0.1452(2)	0.1454(2)	0.4(1)
O2	4j	0.5	0.0	0.0511(3)	0.28(9)	0.0515(3)	0.2(1)	0.0522(3)	0.4(1)	0.0517(3)	0.21(8)	0.0522(3)	0.3(1)	0.0526(2)	0.0522(2)	0.4(1)
O3	4i	0.0	0.5	0.0514(3)	0.3(1)	0.0516(3)	0.2(1)	0.0517(3)	0.3(1)	0.0530(3)	0.27(9)	0.0530(3)	0.3(1)	0.0527(2)	0.0524(2)	0.3(1)
O4	4i	0.0	0.5	0.2182(3)	0.7(3)	0.2183(3)	0.5(3)	0.2184(4)	0.7(1)	0.2177(3)	0.4(1)	0.2177(3)	0.4(1)	0.2182(2)	0.2178(2)	0.8(1)

^a $B_{eq} = \frac{8}{3}\pi^2(U_{11}(aa^*)^2 + U_{22}(bb^*)^2 + U_{33}(cc^*)^2 + 2U_{12}aa^*bb^* \cos \gamma + 2U_{13}aa^*cc^* \cos \beta + 2U_{23}bb^*c^* \cos \alpha)$.

Table 3
Selected interatomic distances for RE124 (Å)

Atoms	YbBa ₂ Cu ₄ O ₈	TmBa ₂ Cu ₄ O ₈	ErBa ₂ Cu ₄ O ₈	HoBa ₂ Cu ₄ O ₈	DyBa ₂ Cu ₄ O ₈	Y _{0.98} Ca _{0.02} Ba ₂ Cu ₄ O ₈
Cu1–Cu1	2.790(2) × 2	2.787(2) × 2	2.788(2) × 2	2.791(2) × 2	2.786(1) × 2	2.792(1) × 2
Cu1–O1	1.838(8)	1.844(9)	1.85(1)	1.818(9)	1.837(5)	1.832(5)
Cu1–O4	1.9349(8) × 2	1.934(1) × 2	1.9358(9) × 2	1.9369(6) × 2	1.9371(6) × 2	1.9365(6) × 2
Cu1–O4	1.870(8)	1.867(9)	1.86(1)	1.884(8)	1.866(5)	1.884(6)
Cu2–O1	2.290(8)	2.274(9)	2.26(1)	2.291(9)	2.264(5)	2.279(5)
Cu2–O2	1.928(1) × 2	1.928(1) × 2	1.928(1) × 2	1.934(1) × 2	1.9326(9) × 2	1.9336(8) × 2
Cu2–O3	1.946(1) × 2	1.945(1) × 2	1.947(1) × 2	1.9459(9) × 2	1.9475(8) × 2	1.9476(8) × 2
Ba–O1	2.731(1) × 4	2.729(1) × 4	2.731(1) × 4	2.738(1) × 4	2.7358(8) × 4	2.7374(7) × 4
Ba–O2	2.969(6) × 2	2.963(6) × 2	2.952(7) × 2	2.969(5) × 2	2.951(3) × 2	2.957(4) × 2
Ba–O3	2.952(6) × 2	2.951(6) × 2	2.952(6) × 2	2.930(6) × 2	2.940(3) × 2	2.943(4) × 2
Ba–O4	2.969(6) × 2	2.967(7) × 2	2.970(7) × 2	2.955(6) × 2	2.963(4) × 2	2.960(4) × 2
RE–O2	2.376(4) × 4	2.381(5) × 4	2.394(5) × 4	2.388(4) × 4	2.401(3) × 4	2.397(3) × 4
RE–O3	2.364(5) × 4	2.369(5) × 4	2.371(5) × 4	2.396(4) × 4	2.390(3) × 4	2.388(3) × 4

An analytical absorption correction was applied to each compound using the linear absorption coefficient given in Table 1, which resulted in the listed transmission factors. Corrections for Lorentz and polarization effects as well as secondary extinction were applied. The structures were refined by direct methods using the Texsan software package [17]. The refinements were performed with the full-matrix least-squares method, and the final cycles converged to give unweighted and weighted agreement factors. The heavy atoms were refined anisotropically (ex-

cept for Cu2 in Tm124). Scattering factors for neutral atoms were taken from Cromer and Waber, as well as the values for $\Delta f'$ and $\Delta f''$ [18]. Anomalous dispersion effects were included in F_{calc} .

2.4. Magnetic measurements

Magnetic measurements were performed on crystals of the six compounds REBa₂Cu₄O₈ (RE = Yb, Tm, Er, Ho, Dy, and Y_{1-x}Ca_x). The data for RE = Yb, Tm, Er, Ho, and Dy crystals along with

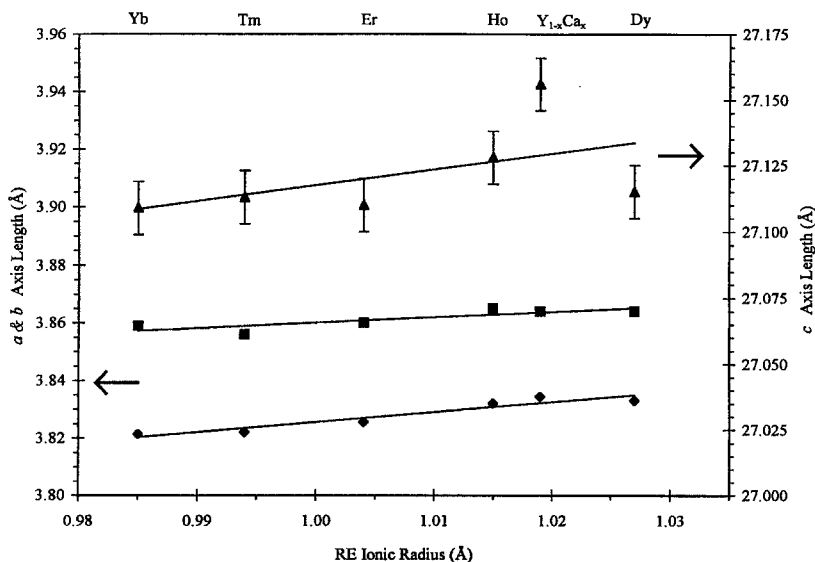


Fig. 1. *a*-, *b*-, and *c*-axis length vs. ionic radius.

data for RE = Y and Gd crystals were reported previously [19]. The $Y_{1-x}Ca_xBa_2Cu_4O_8$ sample was measured using a Lake Shore Cryotronics AC susceptometer at a 1 G field and 100 Hz.

3. Results and discussion

The structure of RE124 consists of a framework of copper–oxygen planes connected by copper–oxygen chains and supported by the rare-earth and barium cations. In the copper–oxygen planes, copper assumes a square pyramidal coordination, while in the chains, copper is found in a square-planar geometry. The rare-earth ions separate two of the planes, and the barium ions are coordinated to the oxygens in the chains and planes. The atomic positions and temperature factors for all six crystals are given in Table 2. The positions for the crystals are almost identical; they differ by at most 3% for the z position. These positions are also similar to those of Y124 [11] and Ca doped Y124 [13]. The temperature factors [B_{eq}] for each of the compounds are very similar. For the calcium-doped sample, the calcium was constrained to the yttrium site and the thermal parameter was equivalent to the yttrium. The selected bond lengths are listed in Table 3. The metal ion–oxygen bond lengths are less reliable because they depend on the accurate determination of the z

parameter for oxygen which is difficult with XRD. The energy dispersive X-ray analysis results verified that the elements present and compositional stoichiometries were correct, and that there was no zirconium from the crucible present in the crystals.

The global structural differences between the RE124 compounds can be observed in the lattice parameters, cell volume, and b/a ratio (the measure of orthorhombic distortion). Table 1 and Figs. 1 and 2 show that as the radius of the lanthanide increased, the size of the lattice parameters and the cell volume increased. The orthorhombic distortion decreased (Fig. 2) with increased RE ion size for RE124. For the rare earth doped 123 compounds, as the lanthanide radius increased, the lattice parameters and volume also increased while the orthorhombic distortion decreased [20]. This size effect for the isoelectronic RE substitution in 124 is larger for the a and b lattice parameters than for the c lattice parameter:

$$\frac{\left(\frac{\Delta a}{a}\right)}{\left(\frac{\Delta R}{R}\right)} = 0.0718, \quad \frac{\left(\frac{\Delta b}{b}\right)}{\left(\frac{\Delta R}{R}\right)} = 0.055,$$

$$\frac{\left(\frac{\Delta c}{c}\right)}{\left(\frac{\Delta R}{R}\right)} = 0.0165;$$

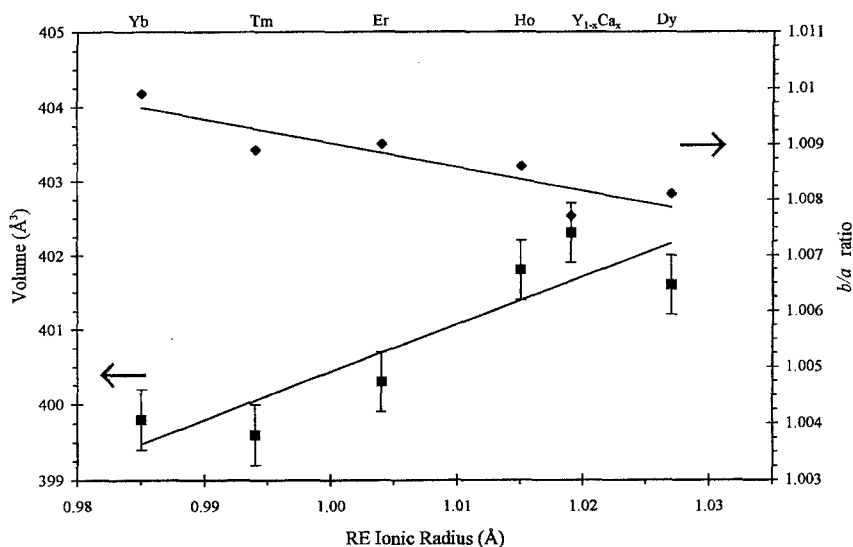


Fig. 2. Cell volume and b/a ratio vs. ionic radius.

R is the ionic radius of the ytterbium cation, and ΔR is the difference between the ionic radii of ytterbium and dysprosium (the largest and smallest cations). The same global effects were observed for powders [6–8]. However, the RE substitution affects only a small part of the lattice along the c -axis, while it influences the a - and b -axes directly. Thus, the better description of structural changes can be obtained by studying the distance between the CuO_2 planes. We find that the change of the Cu–Cu distance out of the CuO_2 plane,

$$\frac{\left(\frac{\Delta d(\text{Cu-Cu})_{\text{out}}}{d(\text{Cu-Cu})_{\text{out}}}\right)}{\left(\frac{\Delta R}{R}\right)} = 0.458,$$

is larger than the change of the Cu–Cu distance in the CuO_2 plane ($= a$ and b). This is consistent with the greater compressibility of the ionic RE–O bonds than the covalent Cu–O bonds.

Fig. 1 shows that the aliovalent Ca^{+2} substitution results in considerable expansion of the c -axis resulting from the increase of the Cu–Cu out of CuO_2 plane distance (Cu2–Cu2 distance = 3.340 Å, c -axis = 27.156 Å). This increase is caused by the substantially larger size of the Ca ion than the Y ion (for eight coordinated $R(\text{Ca}^{+2}) = 1.12$ Å versus $R(\text{Y}^{+3})$

= 1.019 Å). Despite the large increase of the $d(\text{Cu-Cu})_{\text{out}}$, the change of the $d(\text{Cu-Cu})_{\text{in}}$ is minimal. This is the result of two opposite causes: an expansion owing to the size effect and a contraction owing to the hole doping to the anti-bonding Cu–O orbitals. Similar structural changes were observed by Schwer [13] for the Ca doped Y124 grown in Al_2O_3 crucibles.

The refinement of the site occupancies gave a value of 2% for calcium ($x = 0.02$) for the crystal structure of $\text{Y}_{1-x}\text{Ca}_x\text{Ba}_2\text{Cu}_4\text{O}_8$. This value is smaller than the calcium doping levels for the Schwer crystals [13] which range from 3.5 to 6.0%. Our Ca substitution level is also smaller than achieved in powder samples with $x \sim 0.1$ [9]. Stabilization of crystals with a higher calcium content may be accomplished by increasing the amount of calcium in the original reaction mixture and modifying synthesis conditions. Some earlier work concluded that the calcium is substituting on the barium site [21]. For our $\text{Y}_{0.98}\text{Ca}_{0.02}\text{Ba}_2\text{Cu}_4\text{O}_8$ sample, however, the model could not be refined with calcium on the barium site, only with calcium on the yttrium site. This is consistent with recent refinement results of Schwer et al.

A decreasing trend in the T_c with increasing ionic radius was previously noted for RE124 samples [19] and is also presented here in Fig. 3. For RE123, the

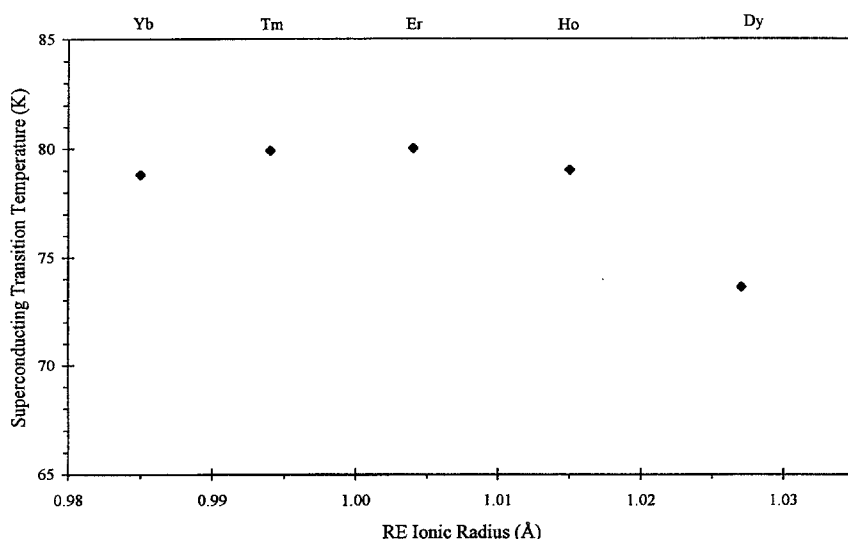


Fig. 3. Superconducting transition temperature vs. ionic radius.

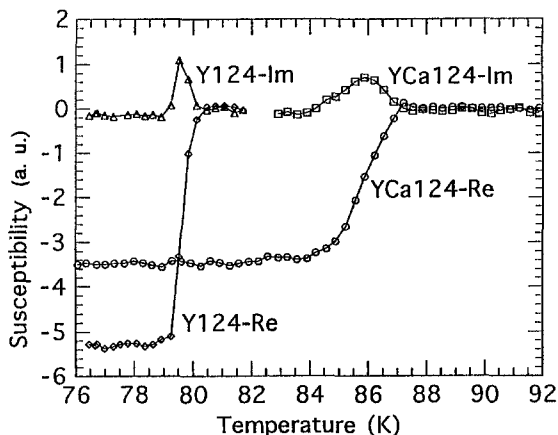


Fig. 4. Magnetic-susceptibility measurements for Y124 and Ca doped Y124 crystals with both the real (Re) and the imaginary (Im) components plotted.

critical temperature increased as the ionic radii of the rare-earth cations increased which is the opposite effect from RE124 [22]. Magnetic susceptibility versus temperature for the doped and undoped Y124 is shown in Fig. 4. The T_c for the calcium doped material is 7 K higher than that for the undoped compound, $T_c \sim 87$ K. These critical temperatures are higher than those reported by Schwer et al. for their calcium-doped single crystals [13]. T_c 's of 77–79 K and 70–73 K were determined for the doped and undoped samples, respectively. The lower T_c 's, as compared to powder samples, were attributed to contamination by aluminum from the crucible. There was no evidence of a similar contamination for our materials. The increase of T_c between doped and undoped Schwer crystals, ~ 7 K, is consistent with our findings. In powder samples, a 10 K increase of T_c was observed when the sample was doped with 10% calcium [9]. Therefore, the maximum calcium doping level for crystals may be lower than that for powder, resulting in a corresponding lower increase in T_c . The increase of T_c is believed to be caused by an increase in the hole concentration [9]. This is supported by structural data which show Ca^{+2} on the Y^{+3} site and a full oxygen stoichiometry of 8. The minimal increase of the a and b lattice parameters with large increase of the c -axis parameter when compared with corresponding RE124 lattice param-

eters indicates hole charge transfer to the CuO_2 planes. Thus, while pure Y124 is known to be underdoped, the Ca doped Y124 is close to the optimally doped high temperature superconductor.

4. Conclusions

Single crystals of $\text{REBa}_2\text{Cu}_4\text{O}_8$ compounds with the lanthanides Yb, Tm, Er, Ho, and Dy can be grown at $\sim 1100^\circ\text{C}$ and 600 bar of O_2 . Calcium-doped $\text{YBa}_2\text{Cu}_4\text{O}_8$ crystals can also be obtained by this method, while we were not able to grow crystals with larger rare earths. These crystals are of an appreciable size and quality to be analyzed by single crystal X-ray diffraction. All compounds fit the structure of $\text{YBa}_2\text{Cu}_4\text{O}_8$, with changes in the lattice parameters and cell volume corresponding to the variation in the ionic radii of the lanthanides. The different lanthanides also give rise to slightly different superconducting transition temperatures, which vary inversely with ionic radius. The calcium-doped compound was found to contain 2% calcium on the Y^{+3} site, and the critical temperature was 87 K, seven degrees higher than the T_c of the undoped compound.

Acknowledgement

This research was supported by the National Science Foundation under Grant No. DMR 91-20000, through the Science and Technology Center for Superconductivity.

References

- [1] G.F. Holland and A.M. Stacy, *Acc. Chem. Res.* 21 (1988) 8.
- [2] C.N.R. Rao, ed., *Chemistry of Oxide Superconductors* (Blackwell, Oxford, 1988).
- [3] J.D. Jorgensen, B.W. Veal, A.P. Paulikas, L.J. Nowicki, G.W. Crabtree, H. Claus and W.K. Kwok, *Phys. Rev. B* 41 (1990) 41.
- [4] J.D. Jorgensen, M.A. Beno, D.G. Hinks, L. Soderholm, K.J. Volin, R.L. Hitterman, J.D. Grace, I.K. Schuller, C.U. Segre, K. Zhang and M.S. Kleefisch, *Phys. Rev. B* 36 (1987) 3608.
- [5] J. Karpinski, E. Kaldis, S. Rusiecki, E. Jilek, P. Fischer, P. Bordet, C. Chaillout, J. Chenavas, J.L. Hodeau and M.J. Marzio, *Less-Common Met.* 150 (1989) 129.

- [6] D.E. Morris, J.H. Nickel, J.Y.T. Wei, N.G. Asmar, J.S. Scott, U.M. Scheven, C.T. Hultgren, A.G. Markelz, J.E. Post, P.J. Heaney, D.R. Veblen and R.M. Hazen, *Phys. Rev. B* 39 (1989) 7347.
- [7] K. Mori, Y. Kawaguchi, T. Ishigake, S. Katano, S. Funahashi and Y. Hamaguchi, *Y. Physica C* 219 (1994) 176.
- [8] S. Adachi, H. Adachi, K. Setsune and K. Wasa, *Physica C* 175 (1991) 523.
- [9] T. Miyatake, S. Gotoh, N. Koshizuka and S. Tanaka, *Nature (London)* 341 (1989) 41.
- [10] P. Bordet, J.L. Hodeau, R. Argoud, J. Muller, M. Marezio, J.C. Martinez, J.J. Prejean, J. Karpinski, E. Kaldis, S. Rusiecki and B. Bucher, *Physica C* 162 (1989) 525.
- [11] B. Dabrowski, K. Zhang, J.J. Pluth, J.L. Wagner and D.G. Hinks, *Physica C* 202 (1992) 271.
- [12] R.M. Hazen, L.W. Finger and D.E. Morris, *Appl. Phys. Lett.* 54 (1989) 1057.
- [13] H. Schwer, E. Kaldis and J.J. Karpinski, *Solid State Chem.* 111 (1994) 96.
- [14] J. Karpinski, S. Rusiecki, E. Kaldis and E.J. Jilek, *Less Comm. Met.* 164&165 (1990) 3.
- [15] J. Karpinski, S. Rusiedki, E. Kaldis, B. Bucher and E. Jilek, *Physica C* 160 (1989) 449.
- [16] P. Fischer, E. Kaldis, J. Karpinski, S. Rusiecki, E. Jilek, V. Trounov and A.W. Hewat, *Physica C* 205 (1993) 259.
- [17] TEXSAN-TEXRAY Structure Analysis Package, Molecular Structure Corporation, 1985.
- [18] D.T. Cromer and J.T. Waber, *International Tables for X-ray Crystallography*, vol. IV (Kynoch, Birmingham, England, 1974) Table 2.2 A and 2.3.1.
- [19] D.H. Nichols, B. Dabrowski, U. Welp and J.E. Crow, *Phys. Rev. B* 49 (1994) 9150.
- [20] R.M. Hazen, in: *Physical Properties of High Temperature Superconductors II*, ed. D.M. Ginsberg (World Scientific, Singapore, 1990).
- [21] I. Mangelschots, M. Mali, J. Roos, H. Zimmerman, D. Brinkmann, S. Rusiecki, J. Karpinski, E. Kaldis and E. Jilek, *Physica C* 172 (1990) 57.
- [22] B. Dabrowski and D.G. Hinks, in: *Proc. Second Annual Conf. on Superconductivity and Its Applications*, Buffalo, 1988, eds. H.S. Kwok and D.T. Shaw (Elsevier, New York, 1988) p. 141.